Enhancing the circular waveguide microresonator temperature measurement sensitivity and accuracy by using liquid crystal gap filling

Igor A. Goncharenko, Marian Marciniak

Enhancing the circular waveguide microresonator temperature measurement sensitivity and accuracy by using liquid crystal gap filling

Igor A. Goncharenko[1] and Marian Marciniak[2,3]

[1] *Institute for Command Engineers of the Ministry of Emergencies, 25 Mashinostroiteley Str., 220118 Minsk, Belarus*
[2] *National Institute of Telecommunications, 1 Szachowa Str., 04 894 Warsaw, Poland*
[3] *Kielce University of Technology, Faculty of Electrical Engineering, Automatics and Computer Science, al. Tysiaclecia Panstwa Polskiego 7, 25-314 Kielce, Poland*
e-mail : M.Marciniak@itl.waw.pl

Manuscript received: 13/10/2014

Abstract

We consider the design methods and principles of operation of a fast-response integrated optical sensor for temperature measurement. The sensitive element consists of a microring resonator based on the double-slot waveguide made from Si_3N_4 and coated on a SiO_2 buffer layer, which is disposed on a silicon substrate. The nematic 5CB liquid crystal (LC) fills the slots of the ring waveguide. The sensor uses only the optical radiation, and the electrical current is not supplied to the measured matter. That allows applying such sensor for measuring the temperature of highly inflammable liquids and gases. The use of the microresonators based on the double-slot waveguides considerably (more than one order of magnitude) increases the sensor sensitivity. The operating speed of the device is defined by the time of establishing the steady-state regime in the ring microresonator and equals to tens of nanoseconds. The measuring device can consist of a large number of such sensing elements that allows simultaneously controlling the temperature in different points of the fluid flow or the matter volume. The sensor has a micrometer size and can be produced by using routine integrated technologies.

1. Introduction

The wide use of automated control and executive systems, application of new technological processes, conversion to flexible manufacturing systems stimulate the development of measuring and sensor devices. Sensors also are important elements of fire alarm and disaster protection systems. In addition to high metrological characteristics sensors have to possess a high reliability, durability, stability, small size, mass and power consumption, compatibility with microelectronic information processing devices [1]. Fiber and integrated optical devices fulfill these requirements in a maximal degree [2].

Waveguide microring resonators are quite challenging candidates for measuiring the temperature variation with high sensitivity [3-8]. In [3] the method of on-line monitoring the variation of the temperature of remote physical objects on the base of waveguide ring microresonators and its schematic structure is proposed. The temperature range measured by the proposed sensor can be as wide as 500 °C for resonators with radius 8 μm. In order to increase the reliability of data communications the sensor output optical signal is converted into digital form. In [4] an approach to the simultaneous measurement of refractive-index and temperature changes using liquid-core silica optical ring resonators is proposed and theoretically demonstrated. The silicon-based optical ring resonator devices that can resolve temperature differences of 1 mK using the traditional wavelength scanning methodology is presented in [5]. Xuhui Yu et al. [6] demonstrate a sensitive birefringent thermometer based on a SiO_2 waveguide ring resonator. The precision of the sensor is improved by a factor of more than 3, compared to the two-beam polarization interferometer, benefiting from the enhanced birefringence effect from the resonances of two polarization modes in the waveguide ring resonator. A surface plasmon polaritons temperature sensor with temperature sensitivity of 1.36nm/°C is described in [7]. The sensor consists of two metal-insulator-metal waveguides coupled to each other by a ring resonator. The transmission properties are numerically simulated by finite element method. The sensing characteristics of such structure are systematically analyzed by investigating the transmission spectrum. The original device for strain sensing was proposed in [8]. The device constitutes an optical resonator formed by inserting a Fiber Bragg Grating in a closed fiber loop. This peculiar feature allows to perform cavity-enhanced, local strain measurements with a reduced sensitivity to environmental perturbations. Because both the strain and temperature variations result in the change of the grating period, this device also could be used for temparature measurements.

An interesting design for sensing purpose is the slot waveguide, which consists of two strips of a high-index material separated by a sub-wavelength low-index (slot) region [9]. By using the electric field discontinuity at the interface between high-index-contrast materials, increased optical intensity concentration in the slot low-index region can be obtained [10]. The unique feature of a slot waveguide combined with a microring resonator has shown a great potential for sensing applications [11,12]. The slot in such waveguide can be filled with a substance, which is sensitive to a defined parameter, thus increasing the sensor sensitivity [13]. In last years waveguides with double-slot have been proposed for sensing applications. It has been shown that microrings on the base of such waveguide can tolerate larger fabrication errors than single-slot ones [14,15].

Refractive indices of a liquid crystal (LC) are fundamentally interesting and practically useful parameters. In addition to the molecular constituents and wavelength, the temperature is the most important factor affecting the LC refractive indices. As the operating temperature changes, the LC refractive indices change considerably [16,17].

In the paper we consider the operation principle of an optical sensor for temperature measurement on the base of ring microresonator made of double-slot waveguides with LC filling and optimization of the sensor structure for the higher sensitivity and accuracy.

2. Structural diagram and principle of operation of the sensor

Figure1 shows the structure of double-slot waveguide ring microresonator. Ring microresonator

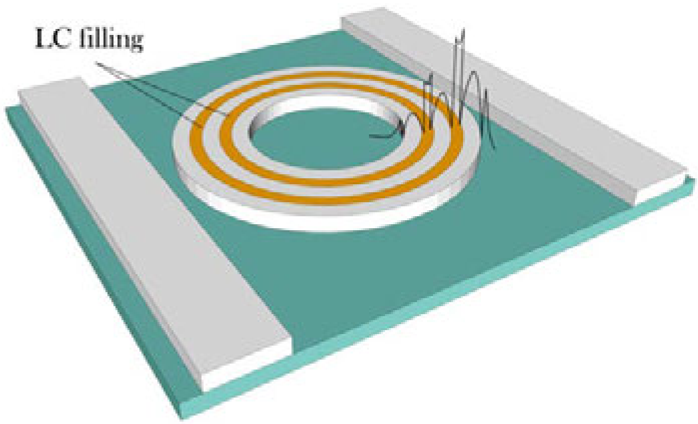

Figure 1. Structure of double-slot waveguide ring microresonator and waveguide mode transverse electric field distribution.

consists of a round optical waveguide with bending radius of the order of tens of microns. Straight optical waveguides coupled with the ring resonator waveguide through evanescent fields are used for input and output of optical signals. The slots of the ring waveguide are filled by liquid crystal. Microresonator is characterized by a set of resonance wavelengths. An input signal on the wavelength coinciding with one of the resonance wavelengths couples into the ring waveguide and passes through it to the output. Any variation of the resonator optical length $L{\cdot}n_{\text{eff}}$, where L is the geometric resonator length, n_{eff} is waveguide mode effective index, leads to shifting its resonance wavelength. As a result the intensity of the output signal on the carrier wavelength coinciding with the resonance wavelength of the unperturbed resonator changes. The operation principle of the sensor is based on changing the waveguide properties of the slot waveguide and consequently the resonance conditions of the microresonator in dependence on index of the LC filling the slot.

We consider waveguides made from Si_3N_4 and coated on a SiO_2 buffer layer, which is disposed on a silicon substrate. The use of Si_3N_4 for the slot-waveguide strips permits a larger slot region to facilitate LC filling of the slot volume [11]. The nematic 5CB liquid crystal fills the slot of the ring waveguide. Microresonator radius is 32 or 16 μm and coupling coefficients between the straight and ring waveguides equal to 0.5. A time of establishing a steady-state condition in the microresonator with such parameters is about 50 ps [18]. This time is one of the aspect that defines the operating speed of the sensor.

The total width of all dielectric strips in the double-slot waveguides is equal 1000 nm. The width of the left G_l and right G_r slots is varied from 50 to 150 nm. The sensitivity of the double-slot waveguide sensors depends on a relative size of its parts [9], thus we calculated double-slot waveguides with a different ratio between the widths of the side and middle strips. The width of the middle strip W_m varies from 200 to 600 nm. Consequently, the width of the side strips W_l and W_r changes from 400 to 200 nm. The height of all strips is 300 nm. The optical radiation wavelength is 1550 nm.

As the radiation source a semiconductor laser can be optimally used, for instance, Mitsubishi Electric Corporation FU-68PDF-V510M61B 1.55 μm DFB-LD module with a polarization maintaining fiber pigtail. The laser output optical power equals to 15 mW and relative intensity noise is −155 dB/Hz. The optical radiation at the output of the ring resonator is measured by a photodetector, for instance, Hamamatsu Corporation G6742-003 InGaAs pin photodiode on a ceramic substrate with a 0.3mm active area [19]. The photodiode sensitivity on the peak sensitivity wavelength 1550 nm is equal to 0.95 A/W and the dark current is 1.5 nA.

3. Calculating the mode fields and optimizing the sensor design

We used the algorithm based on the Method of Lines [20] modified for the structure under investigation for calculation of the mode field distribution and effective index n_{eff} of the bent double-slot waveguides with LC filling.

The temperature variation of n_e and n_o LC indices can be expressed as [16]:

$$\begin{aligned} n_e(T) &\approx n_i + G_e\left(1-\frac{T}{T_c}\right)^{\beta} \\ n_o(T) &\approx n_i - \frac{G_o}{2}\left(1-\frac{T}{T_c}\right)^{\beta} \end{aligned} \tag{1}$$

where n_i is the index of LC in isotropic state, T_c is the clearing point (clearing temperature), β is a material parameter depending on the LC molecular structure, $G_{e,o}$ are proportionality constants for the corresponding waves. For 5CB LC these parameters are: $n_i = 1.5865$, $T_c = 309.3$ K, $\beta = 0.1375$, $G_e = 0.1914$, $G_o = 0.1942$ [16]. The imaginary part κ of the refractive index of 5CB is smaller than 0.02 and does not exhibit appreciable anisotropy [21]. The real and imagenery parts of the refractive index of Si_3N_4 equal to 2.55 and 0.001, respectively. The same parameters for SiO_2 are 1.45 and less than 0.0004 at 20 °C. Thus, the calculated propagation loss in the double-slot LC-filled ring waveguide with bend radius 32 μm is approximatelly 2.16 dB.

Figure 2 shows the transformation of transverse field distribution of the modes polarized along the substrate plane in bent double-slot waveguides with LC filling under changes of the slot separation W_m. Width of the slots is equal to 100 nm. Bend radius is 32 μm. The transverse mode field distribution in bent double-slot waveguides with limiting large (600 nm, curve 3) and small (200 nm, curve 1) slot separations and specific intermediate (320 nm, curve 2) slot separation is shown in figure 3. It follows from the figures that mode field distribution in double-slot waveguide with large slot separation ($W_m > 400$ nm, $W_l = W_r < 300$ nm) looks like a field of a conventional strip waveguide, because the mode is mostly concentrated in wide middle strip of the double-slot waveguide. At that the mode amplitude in the slot regions is small. The mode field distribution of the double-slot waveguide with a moderate specific slot separation ($W_m \approx 320$ nm, $W_l = W_r \approx 340$ nm) looks similar to the supermode of three coupled waveguides, because the all three strips have approximately the same width. At that the mode amplitude in the slot regions is substantially high. For a small slot separation ($W_m < 300$ nm, $W_l = W_r > 350$ nm) the mode field distribution corresponds to the field of two coupled waveguides but with substantial field amplitude in the slot regions. In this case the waveguide mode is concentrated in side strips, which are wider than the middle strip.

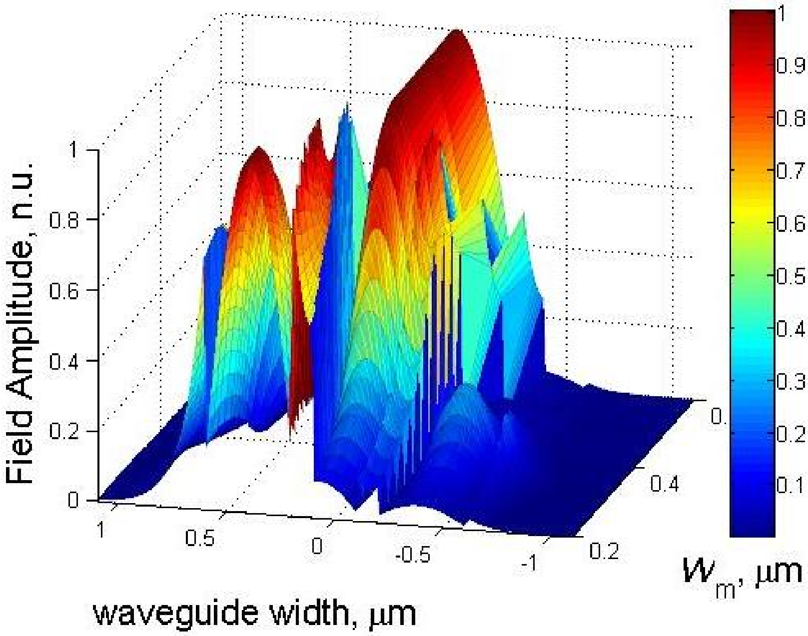

Figure 2. The dependence of the transverse mode field distribution in the bent double-slot waveguides on the slot separation W_m.

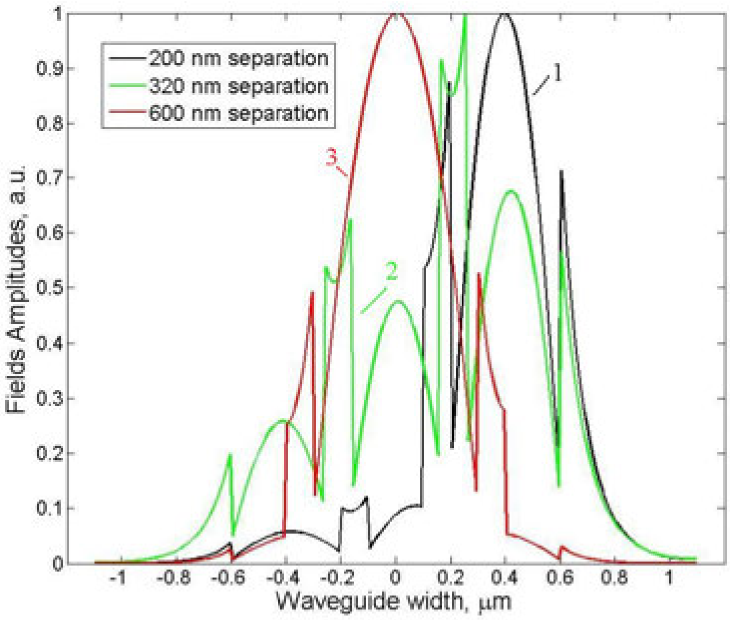

Figure 3. The transverse mode field distribution in the bent double-slot waveguides with LC filling with different slot separation.

The specific slot separation corresponds to the case when all three strips have approximately equal width. In order to check this assumption we have calculated the dependence of the mode field distribution on the slot separation in a double-slot waveguide with a constant width of the side strips. For $W_l = W_r = 300$ nm the specific slot separation equals approximately to 300 nm, whereas for $W_l = W_r = 400$ nm the specific slot separation is achieved with $W_m \approx 400$ nm.

Our calculation shows that the variation of the slot width doesn't influence substantially the mode field distribution in the waveguide regions outside the slots. The slot widening leads only to increasing the part of the optical power in the slot regions. Therefore, one can expect that waveguide with wider slots will be more sensitive to the temperature variation.

Figure 4 shows the optical signal power on the output of the ring resonator with bend radius 32 μm based on double-slot waveguides with a different slot separation. Dashed line 4 presents the optical power on the output of the ring microresonator with bend radius 16 μm based on double-slot waveguide with W_m = 320 nm. It follows from the figure that the ring resonator on the base of double-slot waveguides with the specific medium slot separation ($W_l = W_r \approx W_m$) is the most sensitive to the temperature. At that, the ring resonator with a larger bend radius shows the higher sensitivity to the temperature variation.

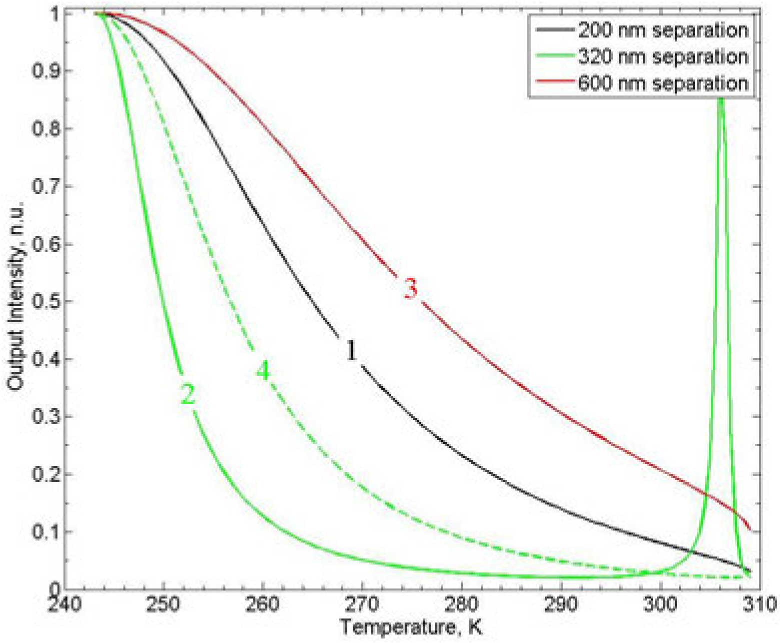

Figure 4. The temperature dependence of optical signal power on the output of ring resonator based on the double-slot waveguides with the slot width $G_l = G_r$ = 100 nm and slot separation W_m equal to 200 (1), 320 (2,4) and 600 (3) nm. Waveguide bend radius is 32 (1-3) and 16 (4) μm.

Using the data from the figure 4 we can estimate the sensor sensitivity to temperature variation. For the laser output optical power 15 mW, photodiode sensitivity 0.95 A/W, 3 dB input/output loss and propagation loss 2 dB, the sensitivity of the sensor based on the waveguide with bend radius 16 μm is equal to 0.14 mA/K in the temperature region from 250 to 270 K and it is 0.04 mA/K for the temperature ranging from 275 to 308 K. The device based on the resonator with radius of 32 μm has the sensitivity to temperature of the order of 0.34 mA/K in temperature range from 245 to 255 K, and only 0.01 mA/K for the temperature from 270 to 295 K.

The operating speed of the device is defined by the time of establishing the steady-state regime in the ring microresonator and the time of response of the sensing element on the temperature variation. The time of establishing the steady-state regime in the ring microresonators with bend radii 8–128 μm is of the order of tens picosecond [18]. The response time of the sensor element $\tau = C/G$, where C is the microresonator thermal capacity, $G = kS_r$ is the heat transfer between resonator and substrate, k is the heat transfer coefficient, S_r is the area of contact between resonator and substrate [22]. Thermal capacity of Si_3N_4 microresonator with bend radius 32 μm, waveguide width 1 μm and thickness 0.3 μm $C \approx 0.128 \cdot 10^{-9}$ Дж·K^{-1}. Heat transfer coefficient for silicon nitride k = 20 W·m^{-2}·K^{-1} [23]. Thus for microresonator with bend radius 32 μm and waveguide width 1 μm the heat transfer between resonator and substrate G is approximately equal to $4.02 \cdot 10^{-9}$ W K^{-1}. Therefore, the characteristic time defining the time of response of the device on the temperature variation τ is equal to 0.032 s.

The measurement range and sensitivity of the temperature sensor on the base of the slot and double-slot waveguide ring microresonator can also be changed by modifying the microresonator parameters, i.e. the ring radius, coupling coefficients, etc. [3,24].

4. Conclusion

We have investigated the structural diagram and the operation principles of an integrated optical temperature sensor. The sensor uses only the optical radiation, and the electrical current is not supplied to the measured matter. That allows to apply such sensor for measuring the temperature of highly inflammable liquids and gases. The use of the microresonators based on the double-slot waveguides considerably (more than one order of magnitude) increases the sensor sensitivity. The operating speed of the device equals to 0.03 s.

The mode field distribution in the double-slot waveguide with an LC filling with a small slot separation is similar to the fields of two coupled waveguides. However the amplitude value in the region of slots is sufficiently large. When the slot separation increases the mode field distribution fluently transforms first to the field of three coupled waveguides, and then converts into the fields of a conventional strip waveguide. It turns out that the largest field amplitude in the slot region corresponds to a moderate slot separation when all three strips of the double-slot waveguide have approximately equal width (the case of three coupled waveguides). As a result, such waveguide is found to be the most sensitive to the temperature changes.

References

[1] Garmash V.B., Egorov F.A., Kolomiets L.N. et. al. Possibilities, tasks and trends of optical fiber measuring systems in modern instrument engineering. *Photon-Express - Science,* **6**, 128–140 (2005).

[2] Passaro V.M.N., Dell'Olio F., Casamassima B. and Leonardis F. De. Guided-wave optical biosensors. *Sensors,* **l7,** 508–536 (2007).

[3] Goncharenko I.A., Esman A.K., Kuleshov V.K. and Pilipovich V.A. A digital optical sensor for the remote monitoring of temperature. *Measurement Techniques.* **50,** 319–324 (2007).

[4] Nai Lin, Lan Jiang, Sumei Wang, Lei Yuan, and Qianghua Chen. Simultaneous measurement of refractive index and temperature using a microring resonator. *Chinese Optics Letters*, **10**, 052802 (2012).

[5] H. Xu, M. Hafezi, J. Fan, J. M. Taylor, G. F. Strouse, and Z. Ahmed. Ultra-sensitive chip-based photonic temperature sensor using ring resonator structures. *Optics Express*. **22**, 3098-3104 (2014).

[6] Xuhui Yu, Huilian Ma, Zhonghe Jin, Ming Pan, Liwei Hou, and Wei Xie. Sensitive birefringent temperature sensor based on a waveguide ring resonator. *Applied Optics*. **53**, 2748-2753 (2014).

[7] Tiesheng Wu, Yumin Liu, Zhongyuan Yu, Yiwei Peng, Changgan Shu, and Han Ye. The sensing characteristics of plasmonic waveguide with a ring resonator. *Optics Express*, **22**, 7669-7677 (2014).

[8] C. E. Campanella, A. Giorgini, S. Avino, P. Malara, R. Zullo, G. Gagliardi, and P. De Natale. Localized strain sensing with fiber Bragg-grating ring cavities. *Optics Express*, **21**, 29435-29441 (2013).

[9] Almeida V.R., Xu Q., Barrios C.A. and Lipson M. Guiding and confining light in void nanostructure. *Opt. Lett*. **29**, 1209–1211 (2004).

[10] Xu Q., Almeida V.R., Panepucci R.R. and Lipson M. Experimental demonstration of guiding and confining light in nanometer-size low-refractive-index material. *Opt. Lett.* **29,** 1626–1628 (2004).

[11] Barrios C.A., Gylfason K.B., Sanchez B., et al. Slot-waveguide biochemical sensor *Opt. Lett*. **32,** 3080–3082 (2007).

[12] Barrios C.A., Banuls K.M.J, Gonzalez-Pedro V., et al. Label-free optical biosensing with slotwaveguides. *Opt. Lett*. **33,** 708–710 (2008).

[13] Goncharenko I. and Marciniak M. Optical temperature sensor on the base of slot waveguide with LC filling. *in Proc*. *ICTON 2012*, Coventry, United Kingdom, paper We.B5.2 (2012).

[14] Dell'Olio F. and Passaro V.M. Optical sensing by optimized silicon slot waveguides. *Opt. Exp*. **15,** 4977–4993 (2007).

[15] Kargar A. and Chung-Yen Chao. Design and optimization of waveguide sensitivity in slot microring sensors. *J. Opt. Soc. Am. A* **28,** 596–603 (2011).

[16] Jun Li and Shin-Tson Wu. Extended Cauchy equations for the refractive indices of liquid crystals. *J. Appl. Phys.* **95,** 896-901 (2004).

[17] Belyaev B.A., Drokin N.A. and Shabanov V.F. Temperature investigation of dielectric characteristics of liquid crystal 5CB in relaxation region. *Solid-state physics.* **47,** 738–741 (2005).
[18] Goncharenko I.A., Esman A.K., Kuleshov V.K. and Pilipovich V.A. Optical broadband analog-digital conversion on the base of microring resonator. *Opt. Commun*. **257,** 54–61 (2006).
[19] http://datasheets.globalspec.com/ds/1031/hamamatsu
[20] Pregla R. The method of lines for the analysis of dielectric waveguide bends. *J. Lightwave Technol.* **14,** 634–639 (1996).
[21] Ru-Pin Pan, Cho-Fan Hsieh, Ci-Ling Pan, Chao-Yuan Chen. Temperature-dependent optical constants and birefringence of nematic liquid crystal 5CB in the terahertz frequency range. *J. Applied Physics*. **103**, paper 093523 (2008).
[22] V.A. Pilipovich, A.K. Esman, I.A. Goncharenko, V.K. Kuleshov. Array converter of infrared images into visible images, based on waveguide microcavities. *J. Optical Technology*. **75**, 333-337 (2008).
[23] T Bechtold, D Hohlfeld, E B Rudnyi and M Günther. Efficient extraction of thin-film thermal parameters from numerical models via parametric model order reduction. *J. Micromechanics and Microengineering*. **20**, paper 045030 (2010).
[24] Goncharenko I.A., Konojko A.I. and Polikanin A.M. Liquid concentration sensor based on slot waveguide microresonators. *Measurement Techniques*. **53**, 563–568 (2010).